Transportation Research Part B 132 (2020) 60–75

Contents lists available at ScienceDirect

Transportation Research Part B

journal homepage: www.elsevier.com/locate/trb

Path-based dynamic pricing for vehicle allocation in ridesharing systems with fully compliant drivers☆

Chao Lei, Zhoutong Jiang, Yanfeng Ouyang*

Department of Civil and Environmental Engineering, University of Illinois at Urbana-Champaign, Urbana, IL 61801, USA

ARTICLE INFO

Article history:
Received 30 November 2018
Accepted 18 January 2019
Available online 19 February 2019

Keywords:
Ridesharing
Dynamic pricing
Self-driving vehicle
Bi-level optimization
MPEC
Approximate dynamic programming

ABSTRACT

Rapidly advancing on-demand ridesharing services, including those with self-driving technologies, hold the promise to revolutionize delivery of mobility. Yet, significant imbalance between spatiotemporal distributions of vehicle supply and travel demand poses a pressing challenge. This paper proposes a multi-period game-theoretic model that addresses dynamic pricing and idling vehicle dispatching problems in the on-demand ridesharing systems with fully compliant drivers/vehicles. A dynamic mathematical program with equilibrium constraints (MPEC) is formulated to capture the interdependent decision-making processes of the mobility service provider (e.g., regarding vehicle allocation) and travelers (e.g., regarding ride-sharing and travel path options). An algorithm based on approximate dynamic programming (ADP), with customized subroutines for solving the MPEC, is developed to solve the overall problem. It is shown with numerical experiments that the proposed dynamic pricing and vehicle dispatching strategy can help ridesharing service providers achieve better system performance (as compared with myopic policies) while facing spatial and temporal variations in ridesharing demand.

1. Introduction

As population and travel demand continue to grow and concentrate into the world's mega cities (Meyer et al., 2012), developing sustainable travel modes for future cities remains a pressing challenge. Yet the average car occupancy (i.e., the number of travelers per vehicle) has been steadily low; e.g., in the U.S. there is only 1.7 passengers per vehicle across all trips and all transportation modes, and this number is even lower for work-based trips (Santos et al., 2011). Such high travel demand, together with low vehicle occupancy, leads to serious traffic congestion in urban areas, and in turn, results in significant losses in travel time, huge wastes of fuel, and large amounts of emissions.

Ridesharing has emerged in many cities as one of the most widely adopted *on-demand* transport modes. In such systems, multiple travelers share a vehicle if their itineraries are spatiotemporally similar. To individual travelers, ridesharing could be attractive because it may help participants substantially reduce their average travel costs, as long as participants can be properly matched, and as long as the service price is lowered to offset the inconvenience of sharing; i.e., leading to "win-win" gains (Chan and Shaheen, 2012; Furuhata et al., 2013). At the system level, ridesharing effectively increases the average vehicle occupancy and reduces the overall vehicle distance traveled to serve the same amount of demand (Fellows

☆ This paper has been accepted for a podium presentation at the 23rd International Symposium on Transportation and Traffic Theory (ISTTT23) July 24–26, 2019 in Lausanne, CH.

* Corresponding author.
E-mail address: yfouyang@illinois.edu (Y. Ouyang).

https://doi.org/10.1016/j.trb.2019.01.017
0191-2615/

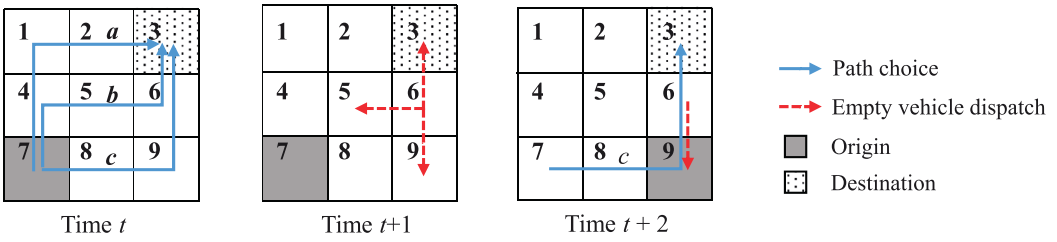

Fig. 1. Illustration of different path choices and vehicle dispatch.

and Pitfield, 2000; International Energy Agency, 2005; Caulfield, 2009; Chan and Shaheen, 2012; Masoud and Jayakrishnan, 2017). Taking the U.S. as an example, the fuel savings from ridesharing was estimated to be up to 5.4% even if one ridesharing occurs to every 10 vehicle trips (Jacobson and King, 2009). The environmental benefits of ridesharing could be more significant for more densely populated cities – it was estimated that ridesharing can help Beijing, China, reduce its annual energy consumption and CO_2 emissions by approximately 26,600 tons-of-coal-equivalent (tce) and 46,200 tons, respectively (Yu et al., 2017).

As a result, the so-called Mobility Service Providers (MSPs), such as Uber and Lyft in the U.S., and DidiChuxing in China, have been experiencing tremendous growth in recent years. Readers can refer to Chan and Shaheen (2012) and Furuhata et al. (2013) for extensive surveys of ridesharing systems. Technologies are instrumental in making ridesharing a reality. For example, GPS-enabled and Internet-accessible smartphones allow the service providers and riders to access their mutual location information instantaneously. Recent advancement of self-driving vehicle technologies are generally expected to play a critical role in the near future – self-driving vehicles are ideal for providing ridesharing service since drivers are no longer part of the picture, and hence the use of vehicles are more flexible and easier to control. Very recently, the potential of dynamic ridesharing with self-driving vehicles in the City of Austin, Texas, is examined by Fagnant and Kockelman (2018) through agent- and network-based simulations. They showed that self-driving ridesharing can benefit both the fleet owner (by bringing more profits) and travelers (by reducing their average waiting and in-vehicle travel times). Hence, it is no surprise that many companies have already planned to launch their self-driving ridesharing pilot programs in cities around the world. Examples include Waymo in Phoenix, Arizona (Korosec, 2017), Lyft in Las Vegas, NV (Shields, 2018), Drive.ai in Frisco, Texas (Ell, 2018), DidiChuxing in China (Campbell and Yang, 2018).

The emerging self-driving technologies (or fully compliant human drivers) allow MSPs to have full control over their vehicles, but yet the travelers make independent decisions on how to travel.[1] There are many opportunities to design proper "mechanisms" to enhance operational efficiency. On the demand side, fare and trip duration are the two leading factors that influence travelers' ridesharing behaviors (Chen et al., 2017). There is an opportunity to influence travelers' decisions by offering a traveler a path option with a relatively longer trip time (e.g., for detouring and serving other passengers) but at a cheaper price. On the supply side, when the spatiotemporal distribution of trip demand is uneven, the MSP may frequently have a need to preposition/dispatch its vehicles to anticipated high-demand areas so as to better capture the demand. For example, as illustrated by the red arrows in Fig. 1, the idling vehicles in area 6 at time $t+1$ can be dispatched to areas 3, 5 or 9 so as to serve demand emerging in those areas at time $t+2$. Some of the current MSPs do this through direct "dispatch orders" (similar to deadheading), which is not productive use of the vehicle resources. In contrast, such "dispatches" can be indirectly achieved via spatiotemporally differential pricing strategies, by allowing vehicles to be rerouted across different paths that pass the desired destinations. For example, in Fig. 1, to serve ride requests from origin area 7 to destination area 3 at time t, the multiple path choices, e.g., path *a, b* and *c* might appear similar. However, if the MSP also knows that high demand from area 9 to area 3 would show up at time $t+2$, it may want to route more vehicles toward area 9. This can be done by adjusting the path prices in advance (i.e., at time t, if it takes one unit of time to travel across one area) to encourage travelers from area 7 to choose path *c* at time t; in turn, more vehicles would be in area 9 at time $t+2$ to provide ridesharing service. This could reduce the need to issue direct "dispatch orders" that are not productive.

In this paper, we focus on investigating (i) how MSPs could use path-based dynamic pricing strategies to influence riders' path choices, (ii) how travelers' decisions would in turn result in reallocation/repositioning of limited ridesharing resource, and meanwhile, (iii) how to dispatch idling vehicle if necessary. One of the major challenges associated with this problem is that the stakeholders of ridesharing systems, usually including both the MSP and individual travelers, exhibit gaming behavior in their decision-making processes. To tackle this challenge, we develop a bi-level game-theoretic model to capture the independent decision-making processes of the stakeholders, where the MSP's path-based pricing and vehicle dispatching decisions are jointly determined in the upper level and the travelers' collective path choices are made in the lower level. The goal of MSPs is to achieve the best utilization of ridesharing vehicle resources to serve spatiotemporally unbalanced demand. The problem is formulated in the form of a multi-period mathematical program with equilibrium constraints

[1] We consider fully compliant drivers (e.g., via self-driving vehicles) to avoid addressing drivers' reactions to pricing/dispatching decisions. In other contexts, the drivers' response to pricing/dispatching decisions need to be explicitly considered in a two-sided market, e.g., drivers may have their own preference in choosing paths, and drivers may refuse to follow the dispatch orders.

(MPEC), and a non-myopic algorithm based on approximate dynamic programming (ADP) is developed to solve the model. The effectiveness and applicability of the proposed model and algorithm are tested through a series of numerical experiments. It is shown that, through path-based pricing policy, the ridesharing systems can achieve much more superior performance as compared with those under alternative policies.

This remainder of the paper is organized as follows. Section 2 gives a review of the relevant literature. Section 3 presents the bi-level MPEC formulation for the proposed path-based dynamic ridesharing pricing problem. Section 4 describes the solution algorithm based on ADP. Section 5 presents numerical experiments that test the applicability and performance of the proposed model. Section 6 concludes the paper and discusses possible directions of future research.

2. Literature review

It is well-known that running a ridesharing system to provide on-demand service is very complicated. In particular, (i) dynamic matching of ridesharing participants and (ii) pricing scheme design are considered to be the two most challenging problems (Furuhata et al., 2013). Despite the rapid growth of the ridesharing market and intensive efforts from the industry, systematic studies of these two problems have attracted attention only in very recent years.

The dynamic rideshare matching problem determines vehicle routes and the assignment of riders to vehicles on short notice such that the ride participants with similar but different itineraries and schedules can be coordinated. The objective includes maximizing the number of serviced riders, minimizing the operating cost of service provider, and minimizing riders' inconvenience. Tackling a practical problem like this, particularly in a dynamic setting, is usually computationally challenging. Agatz et al. (2012) gave the definition of dynamic ridesharing and presented a detailed review of optimization schemes for the dynamic rideshare matching problem. As a representative of this line of studies, Agatz et al. (2011) developed a weighted bipartite matching model to pair drivers and riders dynamically, with the goal of minimizing the total system-wide vehicle miles incurred by system users. They conducted a simulation study based on actual travel data from the Atlanta metropolitan area and showed that the sophisticated optimization methods outperform the simple greedy rules. This problem has also been studied as a number of variants, such as multi-hop Peer-to-Peer (P2P) ride-matching, where multiple riders are allowed to be onboard simultaneously and a rider can transfer between multiple drivers (Cortés et al., 2010; Ghoseiri, 2012; Masoud and Jayakrishnan, 2017), dynamic rideshare matching with dedicated drivers (Lee and Savelsbergh, 2015), the taxi-sharing problem (Hosni et al., 2014), and so on. These studies assume that the matching decision is made centrally by MSPs without considering the fact that travelers are actually heterogeneous and may have their own preferences (e.g., trip duration vs. fare). Moreover, the amount of travelers that are willing to use the ridesharing service is likely to be endogenously related to the ride service quality, e.g., if the fare and service duration go beyond travelers' expectations, they may simply resort to alternative means of transport, such as private vehicle or public transport. As an attempt to overcome these shortcomings, both the heterogeneous and elasticity of ridesharing demand are considered in our study.

The ridesharing pricing problem has received even less attention in the literature. Almost all existing literature related to ridesharing pricing puts attention on a two-sided market, where MSPs offer service to riders via "self-scheduling" drivers who decide for themselves when and how long to work based on the wages that they are paid. One typical objective of this type of ridesharing platforms is to maximize the net profits obtained from the two-sided market, i.e., the difference between the total revenue collected from riders and the total wages paid to drivers. Surge pricing, a variant of the dynamic pricing strategy, has been used as a short-term cure for the imbalance between ride demand and supply (typically drivers) by many ridesharing platforms (Chen and Sheldon, 2015). The way it works is that, when drivers/vehicles in a certain area are in deficit compared to the ride demand, MSPs automatically raise the prices for certain trips by multiplying the regular fare with a multiplier whose value is larger than one, such that more drivers are enticed to enter that area. Banerjee et al. (2015) modeled surge pricing via a threshold-based queuing model where prices are adjusted based on the number of available vehicles in the queue. They concluded that, other than enhancing the robustness of the system, threshold policies cannot improve revenue or welfare compared to static pricing. However, rather than assuming that riders are only sensitive to prices and would abandon their trips if they are not served immediately, Zha et al. (2017) pointed out that the waiting time of riders should be considered as well. Instead of using queuing model, they investigated the performance of surge pricing by proposing a bi-level programming framework, where the upper-level problem determines the prices while the lower-level problem captures drivers' equilibrium work hour choices under either the neoclassical or income-targeting behavioral hypotheses. They found that the platform and drivers could benefit from such pricing strategy while riders may be made worse off with higher prices being enforced. Based on the analytical and numerical results from a stylized model, Cachon et al. (2017) stated that, as labor becomes more expensive, drivers and riders may be both better off with surge pricing as drivers are better utilized and riders can expand access to service during peak demand hours.

The above surge pricing related literature focuses on the role of pricing in handling the temporal imbalance between demand and supply. Yet, the pricing strategy can also be used as a management approach. Bimpikis et al. (2016) explored and demonstrated the benefit of spatial pricing discrimination in a context that ridesharing systems are operated over a network of locations, where the ride demand is heterogeneous in terms of destination preferences and the willingness to pay for service. Luo and Saigal (2017) proposed a continuous-time continuous-space approach to handle the complicated spatiotemporal pricing problem, which allows the agency to determine the optimal prices (to riders) and compensations (to drivers) without suffering from combinatorial complexities.

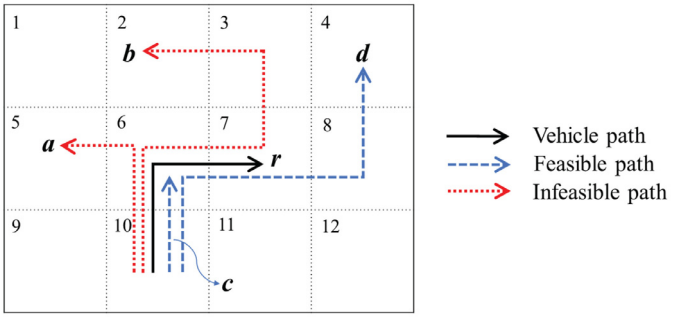

Fig. 2. Illustration of matching rules for different paths ($n = 1$).

It should be noted that our knowledge of how to optimally manage resources in *one-sided* ridesharing systems, even when MSPs have full control over drivers and vehicles, is still quite lacking. The closest literature to our study might be that dynamic pricing for the one-sided ridesharing market, which was recently studied by Qiu et al. (2018). They considered that a monopolistic MSP owns a fleet of identical vehicles and provides two types of on-demand travel services: single or shared, which means travelers can either choose between these two or just reject the service. With the travelers' selection problem being characterized by a probabilistic choice model, a dynamic programming framework was proposed to find the pricing strategy that maximizes the total profit within a specific time horizon. A parametric rollout policy and stochastic optimization approach are developed. They demonstrated that the dynamic pricing policy can generate considerably higher profit than other naive strategies. The major differences between Qiu et al. (2018) and our study are threefold: (i) instead of assuming that the operator has complete knowledge of potential ride requests, we consider both uncertainty and elasticity of ridesharing demand; (ii) instead of assuming that travelers only have mode choices, we consider multiple path options; (iii) instead of only using dynamic pricing strategy to generate profit, we additionally consider how the operator can control the deployment of its vehicles. In our work, an integrated model that combines the dynamic pricing approach and the direct deployment of idling vehicles is proposed to achieve the best performance of ridesharing systems in the context of the one-sided market.

3. Mathematical modeling

In this section, we present a dynamic formulation of a Stackelberg leader-follower game model that determines path-based prices and idling vehicle dispatching strategies for an MSP company in a finite time horizon. The Stackelberg leader-follower game, which has been widely applied to many hierarchical optimization problems in the transportation field (Yang and Bell, 2001; Mackowski et al., 2015; Lei and Ouyang, 2017), is often modeled in the form of MPEC (Luo et al., 1996).

Consider a ridesharing system where users can make real-time ridesharing requests that contain the time of the request and the origin-destination information. For the clarity of illustration, we call each time instant at which the company or users make decision as a decision epoch, and denote all decision epochs as a set $\mathcal{T} = \{0, 1, \ldots, |\mathcal{T}|\}$, where the time interval between any two consecutive decision epochs has the same length Δ. In this study, we assume that the ridesharing requests originate from an urban area with a set of disjointly distributed zones $\mathcal{Z} = \{1, 2, \ldots, |\mathcal{Z}|\}$, as shown in Fig. 2.[2] We consider that the city streets in the studied area form a dense grid network and the zones are rectangular in shape, such that vehicles would move horizontally or vertically across zones.[3] Somewhat similar to the cell transmission model (Daganzo, 1994), we assume that the length of the longest side of a zone should not exceed $\Delta \times v$, where v denotes the average speed of vehicles, such that a vehicle can surely traverse a zone in a single time period. Therefore, instead of considering every single ridesharing request separately, we aggregate them accordingly if they share the same arrival time interval $[t, t + \Delta)$ and origin-destination zones $o, d \in \mathcal{Z}$. As such, based on their OD and value of time information, we can categorize all the ride requests in time interval $[t, t + \Delta)$ into a set of types, denoted by $\mathcal{R}_t, \forall t \in \mathcal{T}$, where we use r as the index, i.e., $r = (o, d)$ for $o, d \in \mathcal{Z}$. The arrival of each type of ride requests is assumed to follow a Poisson process with rate λ_r, and we consider the amount/flow of each type of requests arriving in between time t and $t + \Delta$ as the ridesharing demand for the system during that time interval.

As we consider the ridesharing demand to be elastic, the amount of ride requests for each type of demand is assumed to follow a demand function $H(\cdot)$ of their ride disutility u_r, which is related to the ride payment and the associated total

[2] In this study, we develop a macroscopic zone-based model framework for the ridesharing pricing problem where the details of the road networks are omitted. Similar frameworks have been widely applied by many researchers when studying pricing problems that involve spatial transportation networks, e.g., spatial pricing for ride-sourcing systems (Zha et al., 2018) and urban parking systems (D'Acierno et al., 2006). Also, we expect that the difference between an actual path and the representative "zone path" can be well absorbed by the uncertainty terms in the state transition process (as in Eq. (4)) of the dynamic programming approach.

[3] Hexagonal or elongated hexagonal zones might be beneficial under certain distance metrics; see Xie and Ouyang (2015).

travel time from the origin o to destination d (i.e., the summation of the in-vehicle travel time and the waiting time at the origin before it is picked up). For simplicity, we assume that the demand function $H(\cdot)$ is a linear non-increasing function in the following form:

$$H(u_r) = \hat{A}_r - B_r \cdot u_r,\ \forall t \in \mathcal{T}, r \in \mathcal{R}_t, \tag{1}$$

where $\hat{A}_r$ and B_r denote the maximum amount of the type r demand and the change rate of the demand with respect to the disutility u_r, respectively. Given the assumption of the Poisson arrival process of the ridesharing requests, we can know that $\hat{A}_r$ is actually a random variable following a (truncated) Poisson distribution with parameter $\lambda_r \Delta$.

A ride request is served by first matching it to an "available" vehicle and then the vehicle travels through a specific path (represented by a string of zones) that connects the user's origin zone to its destination zone. Obviously, there might be multiple paths between any pair of zones. Here we assume that only the paths that do not involve any zone-level detours are considered. That means neither vertical nor horizontal overlaps are allowed in a feasible path. For example, if we already have a vehicle with one passenger traveling along path r in Fig. 2, then a second ride request traveling along path c or d (i.e., from zone 10 to zone 6, or from zone 10 to zone 4, respectively) is feasible, whereas path a is infeasible as it would result in horizontal detour for the first passenger by visiting zone 5 and path b is infeasible as it would result in horizontal detour by visiting zone 3 and 7 for the second passenger. We let $\mathcal{K}$ denote the set of all feasible paths between any pair of origin-destination zones.

However, it should be noted that a ridesharing request of a certain type can only be matched to a specific vehicle under some unique conditions. Assume that the MSP company owns and manages a total number of N homogeneous vehicles that share the same maximum passenger capacity $C > 0$.[4] Similarly to the definition of ridesharing demand, we categorize the entire fleet of vehicles into different types based on their specific status. We let $\mathcal{Q}_t$ denote the set of vehicle types at time $t \in \mathcal{T}$, indexed by $q = (l, n, \mathbf{d}, h, \mathbf{s})$, where l denotes the zone where the vehicles are currently located, n denotes the number of onboard passengers, $\mathbf{d}$ is a vector of their destination zones, $h \in \mathcal{K}$ denotes the path that the vehicles would follow to transport the on-board passengers, and $\mathbf{s}$ is a vector that keeps track of the vehicles' estimated arrival time at each zone along path h. As such, the state of vehicles in the system can be represented by the number of type $q \in \mathcal{Q}_t$ vehicles at time $t \in \mathcal{T}$, denoted by $m_{t,q}$.

To this point, we can define the set of vehicle types that are "available" to serve a type $r \in \mathcal{R}_t, \forall t \in \mathcal{T}$ ride request, denoted by $\mathcal{Q}_{t,r}$, as follows:

$$\mathcal{Q}_{t,r} = \{q \in \mathcal{Q}_t | l_q = o_r, n_q < C, \mathcal{K}_{r,q} \neq \emptyset\},\ \forall t \in \mathcal{T}, r \in \mathcal{R}_t, \tag{2}$$

where $\mathcal{K}_{r,q} \subseteq \mathcal{K}$ denotes the set of paths that allow a type $r \in \mathcal{R}_t$ request to be matched with a type $q \in \mathcal{Q}_t$ vehicle. Any path $k \in \mathcal{K}_{r,q}$ shall satisfy the following conditions: (i) the current location of the vehicle (i.e., the first zone in path h_q) and the origin zone of the ride request, o_r, must be the same; (ii) if the vehicle is non-empty (i.e., $1 \leq n_q < C$), a ride request can be matched to the vehicle via path k only if this path is along the direction of the vehicle's predetermined path h_q (e.g., path c and d in Fig. 2). The paths that would result in zone-level detours are excluded (e.g., path a and b in Fig. 2); (iv) for the vehicles that are empty, i.e., $n_q = 0$, $\mathcal{K}_{r,q}$ is a collection of all feasible paths that start from the origin zone o_r and end at its destination zone d_r.

Given the type information of a ride request, the system would automatically check if there are any vehicles are suitable to serve this request based on the pre-constructed set $\mathcal{Q}_{t,r}, \forall t \in \mathcal{T}, r \in \mathcal{R}_t$. It is easy to discover that there might be multiple types of vehicles and multiple possible paths to serve a certain ride request. We assume that the company would post the ride prices for each feasible path, along with its associated arrival time at the destination, to the user who requests ridesharing service via mobile applications. Meanwhile, every user can select one optimal path from all the options based on its own preference/objective. In the following, we present a multi-period bi-level MEPC formulation for the problem, where the MSP company's pricing and vehicle dispatching problem at each decision epoch is in the upper level (see Section 3.1) and the users' collective path choice equilibrium is in the lower level (see Section 3.2).

3.1. Upper level problem

In the upper level, the MSP company acts as a leader and attempts to achieve the best system-wide performance by optimally utilizing the limited vehicles in the system. As mentioned in Section 1, we consider that the company has two approaches to reach its goal: one is that influencing the users' path choices via optimal pricing strategy such that more vehicles can show up in the desired zones to satisfy the upcoming demand, while the other approach is through giving direct orders to the idling vehicles so as to reallocate them to the designated areas.

For the path-based pricing approach, the company needs to determine the prices for each possible path between any pair of zones at each decision epoch $t \in \mathcal{T}$. Let $p_{t,q,k}$ represent the price for using a type $q \in \mathcal{Q}_t$ vehicle to transport a passenger through path $k \in \mathcal{K}_q$, where $\mathcal{K}_q$ is the set of all possible paths that a vehicle of type $q \in \mathcal{Q}_t$ can serve. Let $\mathbf{p}_t :=$

[4] We assume that the size of the ridesharing vehicle fleet is moderate such that the impact of their operations on traffic congestion is negligible. Nevertheless, the proposed approach takes into account the latest traffic condition at each new decision epoch. The homogeneous assumption can easily be relaxed as the heterogeneity of fleet can be incorporated by simply adding more elements into the vehicle type tuple, e.g., the capacity or the type of service that vehicles can provide. In this work we only consider the homogeneous case for simplicity of modeling.

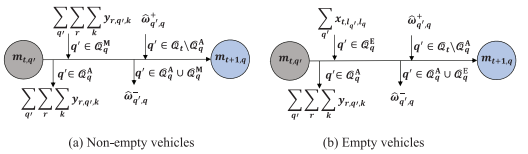

Fig. 3. Transition of vehicle states.

$\left\{p_{t,q,k}|\forall q \in \mathcal{Q}_t, k \in \mathcal{K}_q\right\}$. As such, a pricing decision for the entire planning horizon is then written as $\mathbf{p} = \left\{\mathbf{p}_0, \mathbf{p}_1, \ldots, \mathbf{p}_{|\mathcal{T}|}\right\}$. In practice, ridesharing prices may subject to certain regulations. For example, a "ceiling" value is usually enforced over the price for a specific path, i.e.,

$$\overline{p}_k^{\mathrm{LB}} \le p_{t,q,k} \le \overline{p}_k^{\mathrm{UB}}, \ \forall t \in \mathcal{T}, q \in \mathcal{Q}_t, k \in \mathcal{K}_q, \tag{3}$$

where $\overline{p}_k^{\mathrm{UB}}$ and $\overline{p}_k^{\mathrm{UB}}$ denote the price lower and upper limit of path $k \in \mathcal{K}_q$, respectively.

For the vehicle dispatching approach, the MSP company dispatches the vehicles, which remain idling in certain zones after all the ride requests are served, to some other zones that are in lack of vehicles. We denote the amount/flow of idling vehicles that are dispatched from zone $j \in \mathcal{Z}$ to zone $j' \in \mathcal{Z}_j$ in time interval $[t, t+\Delta)$ as decision variable $x_{t,j,j'}$, where $\mathcal{Z}_j$ represents the set of zones that an empty vehicle originated from zone j can reach to within one time interval.

As time passes, the vehicles of a certain type may evolve into other types by (i) picking up a newly matched passenger, (ii) dropping off an onboard passenger to its destination, or (iii) simply moving from one zone to another. For example, some vehicles of type $q \in \mathcal{Q}_t, \forall t \in \mathcal{T}$ with $n_q = 2, \mathbf{d}_q = \{d_1, d_2\}$ might evolve into vehicles of type $q' \in \mathcal{Q}_{t+1}$ with $n_{q'} = 1, \mathbf{d}_{q'} = \{d_2\}$ if the first passenger is dropped off at zone d_1. The path h_q would be updated to $h_{q'}$ considering that its first zone changes to d_1, and the associated schedule s_q would be updated to $s_{q'}$ considering the time spent in dropping off that passenger. Let $y_{r,q,k}$ denote the amount of type $r \in \mathcal{R}_t, \forall t \in \mathcal{T}$ requests using type $q \in \mathcal{Q}_{t,r}$ vehicles via path $k \in \mathcal{K}_{r,q}$. Meanwhile, the evolution of vehicle status is also under the influence of the exogenous randomness, e.g., the actual arrival process of ride requests, as well as the real-time traffic conditions. Therefore, such information should be incorporated into the transition of the vehicle status. We use $\hat{\omega}^+_{q',q}$ to denote the amount of vehicles that change from type q' to type q merely because of the exogenous randomness, and $\hat{\omega}^-_{q',q}$ the amount of vehicles that are supposed to change from type q' to type q but fail to do so due to the random interference. The conservation constraints of vehicles over one time interval (e.g., from t to $t+1$) can thus be formulated as follows:

$$m_{t+1,q} = \begin{cases} \sum\limits_{q' \in \mathcal{Q}_q^{\mathrm{A}}} \left(m_{t,q'} - \sum\limits_{\substack{r \in \mathcal{R}_t, \\ o_r = l_{q'}}} \sum\limits_{k \in \mathcal{K}_{r,q'}} y_{r,q',k} \right) + \sum\limits_{q' \in \mathcal{Q}_q^{\mathrm{M}}} \sum\limits_{\substack{r \in \mathcal{R}_t, \\ o_r = l_{q'}}} \sum\limits_{k \in \mathcal{K}_{r,q'}} y_{r,q',k} + \sum\limits_{q' \in \mathcal{Q}_t \setminus \mathcal{Q}_q^{\mathrm{A}}} \hat{\omega}^+_{q',q} - \sum\limits_{q' \in \mathcal{Q}_q^{\mathrm{A}} \cup \mathcal{Q}_q^{\mathrm{M}}} \hat{\omega}^-_{q',q}, & \text{if } n_q > 0; \\ \sum\limits_{q' \in \mathcal{Q}_q^{\mathrm{A}}} \left(m_{t,q'} - \sum\limits_{\substack{r \in \mathcal{R}_t, \\ o_r = l_{q'}}} \sum\limits_{k \in \mathcal{K}_{r,q'}} y_{r,q',k} \right) + \sum\limits_{q' \in \mathcal{Q}_q^{\mathrm{E}}} x_{t,l_{q'},l_q} + \sum\limits_{q' \in \mathcal{Q}_t \setminus \mathcal{Q}_q^{\mathrm{A}}} \hat{\omega}^+_{q',q} - \sum\limits_{q' \in \mathcal{Q}_q^{\mathrm{A}} \cup \mathcal{Q}_q^{\mathrm{E}}} \hat{\omega}^-_{q',q}, & \text{otherwise;} \end{cases},$$

$$\forall t \in \mathcal{T} \setminus \{|\mathcal{T}|\}, q \in \mathcal{Q}_{t+1}, \tag{4}$$

where $\mathcal{Q}_q^{\mathrm{M}}$ denotes the set of vehicle types that can evolve into type $q \in \mathcal{Q}_{t+1}$ in one time interval by *matching* new passengers, $\mathcal{Q}_q^{\mathrm{A}}$ denotes the set of vehicle types would *automatically* evolving into type $q \in \mathcal{Q}_{t+1}$ without any matching, and $\mathcal{Q}_q^{\mathrm{E}}$ denotes the set of *empty* vehicles that can be dispatched to zone l_q in one time interval. As shown in Fig. 3, the transition of the vehicle types can be explained as follows: (i) for type $q \in \mathcal{Q}_{t+1}$ vehicles that are not empty at time $t+1$, i.e., $n_q > 0$ (Fig. 3(a)), $m_{t+1,q}$ is calculated by summing up three parts – the number of vehicles that evolve into type q by matching new passengers in time period $[t, t+\Delta)$, i.e., $\sum_{q' \in \mathcal{Q}_q^{\mathrm{M}}} \sum_{r \in \mathcal{R}_t, o_r = l_{q'}} \sum_{k \in \mathcal{K}_{r,q'}} y_{r,q',k}$; the number of vehicles that would automatically evolve into type q without any matching, i.e., $\sum_{q' \in \mathcal{Q}_q^{\mathrm{A}}} \left(m_{t,q'} - \sum_{r \in \mathcal{R}_t, o_r = l_{q'}} \sum_{k \in \mathcal{K}_{r,q'}} y_{r,q',k} \right)$; and the net changes from randomness, i.e., $\sum_{q' \in \mathcal{Q}_t \setminus \mathcal{Q}_q^{\mathrm{A}}} \hat{\omega}^+_{q',q} - \sum_{q' \in \mathcal{Q}_q^{\mathrm{A}} \cup \mathcal{Q}_q^{\mathrm{M}}} \hat{\omega}^-_{q',q}$; (ii) for those vehicles that are empty at time $t+1$, i.e., $n_q = 0$ (Fig. 3(b)), they can only come from the ones that would automatically evolve to type q vehicles; the empty vehicles that were repositioned to zone l_q in time period $[t, t+\Delta)$, i.e., $\sum_{q' \in \mathcal{Q}_q^{\mathrm{E}}} x_{t,l_{q'},l_q}$; and again, the net change due to random interference, i.e., $\sum_{q' \in \mathcal{Q}_t \setminus \mathcal{Q}_q^{\mathrm{A}}} \hat{\omega}^+_{q',q} - \sum_{q' \in \mathcal{Q}_q^{\mathrm{A}} \cup \mathcal{Q}_q^{\mathrm{E}}} \hat{\omega}^-_{q',q}$. Note that the total number of empty vehicles that can be sent out from zone $j \in \mathcal{Z}$ should be no greater than the number of vehicles that remain idling in zone j, i.e.,

$$\sum_{j' \in \mathcal{Z}_j} x_{t,j,j'} = m_{t,q} - \sum_{\substack{r \in \mathcal{R}_t, \\ o_r = l_q}} \sum_{k \in \mathcal{K}_{r,q}} y_{r,q,k}, \forall t \in \mathcal{T}, j \in \mathcal{Z}, n_q = 0, l_q = j. \tag{5}$$

The objective of the MSP is usually to maximize the collected revenue while minimizing the total operating costs. However, it should be noted that, for the on-demand ridesharing systems operated with a reasonably small fleet size, the vehi-

cles tend to keep moving. As such, the overall operating time/cost during the planning horizon is approximately a constant value and thus can be omitted in the objective function. The primary objective of the MSP company is thus to maximize the expected total revenue over the entire planning horizon as follows:

$$\max_{\mathbf{p},\mathbf{x}} \mathbb{E}\left\{ \sum_{t=0}^{|\mathcal{T}|} \gamma^t G_t(\mathbf{m}_t, \mathbf{p}_t, \mathbf{x}_t) \middle| \mathbf{m}_0 \right\}, \tag{6}$$

where $\overline{\mathbf{m}}_0$ denotes the initial location and occupancy state of all the vehicles, $\gamma \in [0, 1]$ denotes a temporal discounting factor, and $G_t(\mathbf{m}_t, \mathbf{p}_t, \mathbf{x}_t)$ denotes the objective function at decision epoch t, which is defined as

$$G_t(\mathbf{m}_t, \mathbf{p}_t, \mathbf{x}_t) = \sum_{r\in\mathcal{R}_t} \sum_{q\in\mathcal{Q}_{t,r}} \sum_{k\in\mathcal{K}_{r,q}} p_{t,q,k} \cdot y_{r,q,k} \tag{7}$$

Given the path-based prices determined in the upper level, the ridesharing users would then make their choices accordingly such that their own benefits can be maximized. Therefore, how the vehicles and ride requests are matched, i.e., how the decisions $y_{r,q,k}, \forall r \in \mathcal{R}_t, q \in \mathcal{Q}_{t,r}, k \in \mathcal{K}_{r,q}$ are made, would depend on users' optimization problem, which is discussed below as the lower level model.

3.2. Lower level problem

In the lower level, each ridesharing service user acts as a follower and makes his/her own optimal decision while competing against each other for limited vehicles at each decision epoch. All the users are assumed to be rational, attempting to minimize the generalized (time and monetary) costs of using ridesharing service. In a busy urban area, we assume that the users make the ridesharing requests simultaneously in each time interval through mobile applications or other online systems. Hence, we consider that the users' behaviors satisfy a type of Nash equilibrium (Sheffi, 1985; Bai et al., 2016). As such, the company's pricing scheme at each decision epoch can be considered to be effective in adjusting the ridesharing demand. Note that all the type $r \in \mathcal{R}_t, \forall t \in \mathcal{T}$ users should share the same ride disutility u_r when the system is at equilibrium.

The total generalized cost for a type $r \in \mathcal{R}_t$ rider to take a type $q \in \mathcal{Q}_{t,r}$ vehicle via path $k \in \mathcal{K}_{r,q}$, denoted by $\phi_{r,q,k}$, is the summation of the ride payment $p_{t,q,k}$ and the monetary cost for the time spent in taking the ride. Let $D_{r,q,k}$ denote the estimated duration of the ride, which includes both the line-haul travel time and the detour time incurred by picking up or dropping off passengers (including the user itself) along the trip. The formulation of $\phi_{r,q,k}$ can thus be written as

$$\phi_{r,q,k} = p_{t,q,k} + \alpha \cdot D_{r,q,k}, \ \forall r \in \mathcal{R}_t, q \in \mathcal{Q}_{t,r}, k \in \mathcal{K}_{r,q}, \tag{8}$$

where α denotes the monetary value for one unit of time for riders.

Due to the possibility of that not all the ride requests can be accommodated by the limited number of vehicles, we introduce a dummy vehicle type ζ to absorb all the excessive ride requests.[5] It should be noted that a ride request can be assigned to a "dummy" type vehicle only if there are no regular vehicles that are feasible to serve it. In other words, the total cost for using a dummy vehicle must be set higher than the costs for using any regular vehicles, but no higher than the maximum ride disutility value determined by the demand curve, i.e., $H^{-1}(0)$. Thus, the disutility for type $r \in \mathcal{R}_t$ user using the dummy vehicle ζ is defined as

$$\Phi_{r,\zeta} = \min\left\{ H^{-1}(0), \max_{q\in\mathcal{Q}_{t,r}, k\in\mathcal{K}_{r,q}} \left\{ p_k^{\mathrm{UB}} + \alpha \cdot D_{r,q,k} \right\} + \epsilon \right\}, \ \forall t \in \mathcal{T}, r \in \mathcal{R}_t, \tag{9}$$

where ϵ is a constant value larger than 0. Thus, denoting the amount of type $r \in \mathcal{R}_t$ demand being absorbed by the dummy vehicle as $y_{r,\zeta}$, we can formulate the market clearing constraints as

$$H_r(u_r) = \sum_{q\in\mathcal{Q}_{t,r}} \sum_{k\in\mathcal{K}_{r,q}} y_{r,q,k} + y_{r,\zeta}, \ \forall t \in \mathcal{T}, r \in \mathcal{R}_t. \tag{10}$$

In the following, we attempt to derive the equilibrium constraints for the lower level problem by following the similar idea in Mackowski et al. (2015). Let $\mathcal{I}_r$ denote the set of type $r \in \mathcal{R}_t$ users. We define the ride decision of an individual user $i \in \mathcal{I}_r$ as $z_{i,q,k}$, which equals to 1 if user i chooses to take the ride from a vehicle of type $q \in \mathcal{Q}_t$ through path $k \in \mathcal{K}_{r,q}$, or 0 otherwise. Then, the path choice problem for user $i \in \mathcal{I}_r$ can be formulated as follows:

$$\min \sum_{q\in\mathcal{Q}_t} \sum_{k\in\mathcal{K}_{r,q}} \phi_{r,q,k} \cdot z_{i,q,k} + \Phi_{r,\zeta} \cdot z_{i,\zeta} \tag{11}$$

$$\text{s.t.} \sum_{q\in\mathcal{Q}_{t,r}} \sum_{k\in\mathcal{K}_{r,q}} z_{i,q,k} + z_{i,\zeta} = 1, \tag{12}$$

[5] Users could be "lost" to other transport modes (e.g., public transit systems, private cars) if they cannot find desirable ridesharing service. The term ϵ in Eq. (8) can as well serve the purpose of penalizing the system for losing demand to other transportation modes; e.g., if riders are rejected for ridesharing service (i.e., being assigned to dummy vehicles), they may become less willing to use the system.

$$\sum_{k\in\mathcal{K}_{r,q}} z_{i,q,k} + \sum_{r'\in\mathcal{R}_{t,q}} \sum_{\substack{i'\in I_{r'},\\ i'\neq i}} \sum_{k'\in\mathcal{K}_{r',q}} z_{i',q,k'} \le m_{t,q},\ \ \forall q \in \mathcal{Q}_{t,r}, \tag{13}$$

$$z_{i,\zeta}, z_{i,q,k} \in \{0,1\},\ \forall q \in \mathcal{Q}_{t,r}, k \in \mathcal{K}_{r,q}, \tag{14}$$

where $\mathcal{R}_{t,q}$ denotes the set of ride request types that can be served by a type $q \in \mathcal{Q}_t$ vehicle, i.e.,

$$\mathcal{R}_{t,q} = \{r \in \mathcal{R}_t | o_r = l_q, \mathcal{K}_{r,q} \neq \emptyset\},\ \forall t \in \mathcal{T}, q \in \mathcal{Q}_t, n_q < C, \tag{15}$$

The objective function (11) is to minimize the user's total ridesharing cost. Constraint (12) ensures that each ride request is either assigned to a path of an available vehicle or to the dummy vehicle. Constraints (13) state that all the users whose path choices have overlaps with that of user i would compete for the limited vehicles together. Constraints (14) state the binary nature of the decision variables. As problem (11)–(14) fits the special structure of totally unimodular assignment problem, the binary constraints (14) can actually be relaxed into the following form:

$$0 \le z_{i,\zeta} \le 1, \tag{16}$$

$$0 \le z_{i,q,k} \le 1, \forall q \in \mathcal{Q}_{t,r}, k \in \mathcal{K}_{r,q}. \tag{17}$$

Let ψ_i, $\eta_{t,q}$, $\mu_{i,\zeta}$ and $\mu_{i,q,k}$ denote the dual multipliers for constraints (12), (13), (16) and (17), respectively. The Lagrangian function for the optimization problem (11)–(17) can therefore be written as

$$\begin{aligned} L(\psi,\eta,\mu) = &\sum_{q\in\mathcal{Q}_{t,r}} \sum_{k\in\mathcal{K}_{r,q}} \phi_{r,q,k}\cdot z_{i,q,k} + \Phi_{r,\zeta}\cdot z_{i,\zeta} - \psi_i\left(\sum_{q\in\mathcal{Q}_{t,r}} \sum_{k\in\mathcal{K}_{r,q}} z_{i,q,k} + z_{i,\zeta} - 1\right) \\ &+ \sum_{q\in\mathcal{Q}_{t,r}} \eta_{t,q}\left(\sum_{k\in\mathcal{K}_{r,q}} z_{i,q,k} + \sum_{r'\in\mathcal{R}_{t,q}} \sum_{\substack{i'\in I_{r'},\\ i'\neq i}} \sum_{k'\in\mathcal{K}_{r',q}} z_{i',q,k'} - m_{t,q}\right) + \sum_{q\in\mathcal{Q}_{t,r}} \sum_{k\in\mathcal{K}_{r,q}} \mu_{i,q,k}\left(z_{i,q,k}-1\right) + \mu_{i,\zeta}\left(z_{i,\zeta}-1\right). \end{aligned} \tag{18}$$

The first-order KKT conditions are presented as follows:

$$0 \le z_{i,q,k} \perp \left(\phi_{r,q,k} - \psi_i + \eta_{t,q} + \mu_{i,q,k}\right) \ge 0,\ \ \forall q \in \mathcal{Q}_{t,r},\ \ k \in \mathcal{K}_{r,q}, \tag{19}$$

$$0 \le z_{i,\zeta} \perp \left(\Phi_{r,\zeta} - \psi_i + \mu_{i,\zeta}\right) \ge 0, \tag{20}$$

$$0 \le \eta_{t,q} \perp \left(m_{t,q} - \sum_{k\in\mathcal{K}_{r,q}} z_{i,q,k} - \sum_{r'\in\mathcal{R}_{t,q}} \sum_{\substack{i'\in I_{r'},\\ i'\neq i}} \sum_{k'\in\mathcal{K}_{r',q}} z_{i',q,k'}\right) \ge 0,\ \ \forall q \in \mathcal{Q}_{t,r}, \tag{21}$$

$$\psi_i \perp \left(1 - \sum_{q\in\mathcal{Q}_{t,r},\ k\in\mathcal{K}_{r,q}} \sum z_{i,q,k} - z_{i,\zeta}\right) = 0, \tag{22}$$

$$0 \le \mu_{i,q,k} \perp \left(1 - z_{i,q,k}\right) \ge 0,\ \forall q \in \mathcal{Q}_{t,r}, k \in \mathcal{K}_{r,q}, \tag{23}$$

$$0 \le \mu_{i,\zeta} \perp \left(1 - z_{i,\zeta}\right) \ge 0. \tag{24}$$

Since $\mu_{i,q,k} = 0$ and $\mu_{i,\zeta} = 0$ is always feasible to the above KKT conditions, we can simplify (19), (20), (23) and (24) as follows:

$$0 \le z_{i,q,k} \perp \left(\phi_{r,q,k} - \psi_i + \eta_{t,q}\right) \ge 0,\ \ \forall q \in \mathcal{Q}_{t,r},\ \ k \in \mathcal{K}_{r,q}, \tag{25}$$

$$0 \le z_{i,\zeta} \perp \left(\phi_{r,q,k} - \psi_i\right) \ge 0, \tag{26}$$

$$z_{i,\zeta} \le 1 \text{ and } z_{i,q,k} \le 1,\ \ \forall q \in \mathcal{Q}_{t,r},\ \ k \in \mathcal{K}_{r,q}. \tag{27}$$

Based on the postulation that the same type of users share the same ride disutility, i.e., $\psi_i = \psi_{i'} = u_r, \forall i' \in \mathcal{I}_r$, we can sum up (25) and (26) over $\mathcal{I}_r$, and obtain the equilibrium constraints for the lower level problem at decision epoch $t \in \mathcal{T}$, as follows:

$$0 \le y_{r,q,k} \perp \left(\phi_{r,q,k} - u_r + \eta_{t,q}\right) \ge 0, \ \forall r \in \mathcal{R}_t, q \in \mathcal{Q}_{t,r}, k \in \mathcal{K}_{r,q}, \tag{28}$$

$$0 \le y_{r,\zeta} \perp \left(\Phi_{r,\zeta} - u_r\right) \ge 0, \ \forall r \in \mathcal{R}_t, \tag{29}$$

$$0 \le \eta_{t,q} \perp \left(m_{t,q} - \sum_{r \in \mathcal{R}_{t,q}} \sum_{k \in \mathcal{K}_{r,q}} y_{r,q,k}\right) \ge 0, \ \forall q \in \mathcal{Q}_t, \tag{30}$$

$$u_r \perp \left[H(u_r) - \left(\sum_{q \in \mathcal{Q}_{t,r}} \sum_{k \in \mathcal{K}_{r,q}} y_{r,q,k} + y_{r,\zeta}\right)\right] = 0, \ \forall r \in \mathcal{R}_t, \tag{31}$$

where $y_{r,q,k} = \sum_{i \in \mathcal{I}_r} z_{i,q,k}, \ \forall r \in \mathcal{R}_t, q \in \mathcal{Q}_{t,r}, k \in \mathcal{K}_{r,q}$.

As such, the integrated multi-period MPEC formulation of the dynamic ridesharing pricing and vehicle dispatching problem can be obtained:

$$\max_{\mathbf{p},\mathbf{x}} \mathbb{E}\left\{\sum_{t=0}^{T} \gamma^t G_t(\mathbf{m}_t, \mathbf{p}_t, \mathbf{x}_t) \middle| \overline{\mathbf{m}}_0\right\} \tag{32}$$

s.t. (3)–(5), (7), (10), (28)–(30).

4. Solution approach

One typical approach to solving such a multi-period problem like (32) is dynamic programming (DP). Considering each decision epoch $t \in \mathcal{T}$ as a *stage*, the status of vehicle resources and ride requests ($\mathbf{m}_t$, $H_t(u)$) as the *state* of the system, and conservation constraints (4) as the *transition functions*, the Bellman's optimality equation of the dynamic system can be written as

$$V_t(\mathbf{m}_t) = \max_{\mathbf{p}_t} \mathbb{E}\{G_t(\mathbf{m}_t, \mathbf{p}_t, \mathbf{x}_t) + \gamma V_{t+1}(\mathbf{m}_{t+1})\}, \forall \mathbf{m}_t, t \in \mathcal{T}, \tag{33}$$

where $V_t(\mathbf{m}_t)$ denotes the value function of state $\mathbf{m}_t$. However, due to the huge size of the state space and the inherent complexity of MPEC problem, it is almost impossible to solve (33) directly through backward recursion. Therefore, we propose an ADP-based approach (Powell, 2011; Lei and Ouyang, 2017) to tackle this problem.

We present the algorithm framework of the ADP in pseudocode as Algorithm 1 in Appendix A. Specifically, to capture the decreasing marginal value of the vehicle resources, we employ a concave piecewise linear function as the VFA for the ADP approach. The VFA, denoted by $\overline{V}_t(\mathbf{m}_t)$, is defined as the summation of a group of one-dimensional concave separable piecewise linear function of state variables, denoted by $\overline{V}_{t,q}(m_{t,q}), \forall q \in \mathcal{Q}_t$, i.e.,

$$\overline{V}_t(\mathbf{m}_t) = \sum_{q \in \mathcal{Q}_t} \overline{V}_{t,q}(m_{t,q}), \forall t \in \mathcal{T},$$

where the breakpoints of the piecewise linear function $\overline{V}_{t,q}(m_{t,q})$ only occur at integer values of $m_{t,q}$. To avoid the need to approximate the expectation explicitly within the optimization problem, we choose to apply VFA to the post-decision state variables in the objective of the one-stage problem (Powell, 2011). The post-decision state variables, denoted by $m_t^{a,n}$, can be defined as

$$m_{t,q}^a = \begin{cases} \sum_{q' \in \mathcal{Q}_q^{\mathrm{A}}} \left(m_{t,q'} - \sum_{\substack{r \in \mathcal{R}_t, \\ o_r = l_{q'}}} \sum_{k \in \mathcal{K}_{r,q'}} y_{r,q',k}\right) + \sum_{q' \in \mathcal{Q}_q^{\mathrm{M}}} \sum_{\substack{r \in \mathcal{R}_t, \\ o_r = l_{q'}}} \sum_{k \in \mathcal{K}_{r,q'}} y_{r,q',k}, & \text{if } n_q > 0; \\ \sum_{q' \in \mathcal{Q}_q^{\mathrm{A}}} \left(m_{t,q'} - \sum_{\substack{r \in \mathcal{R}_t, \\ o_r = l_{q'}}} \sum_{k \in \mathcal{K}_{r,q'}} y_{r,q',k}\right) + \sum_{q' \in \mathcal{Q}_q^{\mathrm{E}}} x_{t,l_{q'},l_q}, & \text{otherwise;} \end{cases} \quad , \forall t \in \mathcal{T}, q \in \mathcal{Q}_t. \tag{34}$$

Nevertheless, the one-stage subproblem is still computationally challenging because of the bilinear term in the objective function (7) and the involvement of the complementarity constraints (28)–(30). Based on the derivations in Appendix B, we successfully transfer the bilinear term into a concave quadratic form, as follows:

$$\sum_{r \in \mathcal{R}_t} \sum_{q \in \mathcal{Q}_{t,r}} \sum_{k \in \mathcal{K}_{r,q}} p_{t,q,k} \cdot y_{r,q,k} = \sum_{r \in \mathcal{R}_t} H(u_r) \cdot u_r - \sum_{r \in \mathcal{R}_t} \Phi_{r,\zeta} \cdot y_{r,\zeta} - \sum_{q \in \mathcal{Q}_t} m_{t,q} \cdot \eta_{t,q} - \sum_{r \in \mathcal{R}_t} \sum_{q \in \mathcal{Q}_{t,r}} \sum_{k \in \mathcal{K}_{r,q}} \alpha \cdot D_{r,q,k} \cdot y_{r,q,k}. \tag{35}$$

For the complementarity constraints (28)–(30), we reformulate them into a group of mixed-integer linear constraints by introducing an additional binary variable for each complementarity constraint (Hu et al., 2008; Gabriel and Leuthold, 2010; Bai et al., 2012; 2016; Lei and Ouyang, 2017). Define $\xi_{r,q,k}$, $\delta_{r,\zeta}$, $\pi_{t,q} \in \{0, 1\}$ as the indicator variables with respect to constraints (28)–(30), the reformulation of KKT conditions can be thus presented as

$$0 \le y_{r,q,k} \le \overline{y}^{\mathrm{UB}}_{r,q,k} \cdot \left(1 - \xi_{r,q,k}\right),\ \forall r \in \mathcal{R}_t, q \in \mathcal{Q}_{t,r}, k \in \mathcal{K}_{r,q}, \tag{36}$$

$$0 \le \left(\phi_{r,q,k} - u_r + \eta_{t,q}\right) \le \left(\phi^{\mathrm{UB}}_{r,q,k} - \overline{u}^{\mathrm{LB}}_r + \eta^{\mathrm{UB}}_{t,q}\right) \cdot \xi_{r,q,k},\ \forall r \in \mathcal{R}_t, q \in \mathcal{Q}_{t,r}, k \in \mathcal{K}_{r,q} \tag{37}$$

$$0 \le y_{r,\zeta} \le \overline{y}^{\mathrm{UB}}_{r,\zeta} \cdot \left(1 - \delta_{r,\zeta}\right),\ \forall r \in \mathcal{R}_t, \tag{38}$$

$$0 \le \left(\Phi_{r,\zeta} - u_r\right) \le \left(\overline{u}^{\mathrm{UB}}_r - \overline{u}^{\mathrm{LB}}_r\right) \cdot \delta_{r,\zeta},\ \forall r \in \mathcal{R}_t, \tag{39}$$

$$0 \le \eta_{t,q} \le \eta^{\mathrm{UB}}_{t,q} \cdot (1 - \pi_{t,q}),\ \forall q \in \mathcal{Q}_t, \tag{40}$$

$$m_{t,q} \cdot (1 - \pi_{t,q}) \le \sum_{r \in \mathcal{R}_{t,q}} \sum_{k \in \mathcal{K}_{r,q}} y_{r,q,k} \le m_{t,q},\ \forall q \in \mathcal{Q}_t \tag{41}$$

$$\overline{u}^{\mathrm{LB}}_r \le u_r \le \overline{u}^{\mathrm{UB}}_r,\ \forall r \in \mathcal{R}_t, \tag{42}$$

$$H(u_r) = \sum_{q \in \mathcal{Q}} \sum_{k \in \mathcal{K}_{r,q}} y_{r,q,k} + y_{r,\zeta},\ \forall r \in \mathcal{R}_t, \tag{43}$$

$$\xi_{r,q,k}, \delta_{r,\zeta}, \pi_{t,q} \in \{0, 1\},\ \forall r \in \mathcal{R}_t, q \in \mathcal{Q}_{t,r}, k \in \mathcal{K}_{r,q}, \tag{44}$$

where D^{UB}_r, D^{LB}_r, $\overline{u}^{\mathrm{UB}}_r$, $\overline{u}^{\mathrm{LB}}_r$, $\overline{y}^{\mathrm{UB}}_{r,q,k}$, $\overline{y}^{\mathrm{UB}}_{r,\zeta}$ and $\overline{\eta}^{\mathrm{UB}}_{t,q}$ denote the valid upper and lower bounds for $D_{r,q,k}$, u_r, $y_{r,q,k}$, $y_{r,\zeta}$ and $\eta_{t,q}$, which are respectively defined as follows:

$$\left(D^{\mathrm{UB}}_r, D^{\mathrm{LB}}_r\right) = \left(\max_{\substack{q \in \mathcal{Q}_{t,r},\\ k \in \mathcal{K}_{r,q}}} \left\{D_{r,q,k}\right\}, \min_{\substack{q \in \mathcal{Q}_{t,r},\\ k \in \mathcal{K}_{r,q}}} \left\{D_{r,q,k}\right\} \right),\ \forall r \in \mathcal{R}_t, \tag{45}$$

$$\left(\overline{u}^{\mathrm{UB}}_r, \overline{u}^{\mathrm{LB}}_r\right) = \left(\min\left\{ H^{-1}(0), \max_{k \in \mathcal{K}_r} \left\{\overline{p}^{\mathrm{UB}}_k\right\} + D^{\mathrm{UB}}_r + \epsilon \right\}, \min_{k \in \mathcal{K}_r} \left\{\overline{p}^{\mathrm{LB}}_k\right\} + D^{\mathrm{LB}}_r \right),\ \forall r \in \mathcal{R}_t. \tag{46}$$

$$\overline{y}^{\mathrm{UB}}_{r,q,k} = \min\left\{H\left(\overline{u}^{\mathrm{LB}}_r\right), m_{t,q}\right\},\ \forall r \in \mathcal{R}_t, q \in \mathcal{Q}_{t,r}, k \in \mathcal{K}_{r,q} \tag{47}$$

$$\overline{y}^{\mathrm{UB}}_{r,\zeta} = H\left(\overline{u}^{\mathrm{LB}}_r\right),\ \forall r \in \mathcal{R}_t, \tag{48}$$

$$\eta^{\mathrm{UB}}_{t,q} = \max_{r \in \mathcal{R}_{t,q}} \left\{\overline{u}^{\mathrm{UB}}_r - \overline{u}^{\mathrm{LB}}_r\right\},\ \forall q \in \mathcal{Q}_t. \tag{49}$$

At this point, we can present the reformulated one-stage model mentioned in step 5 of Algorithm 1 in Appendix A as follows:

$$\max_{\mathbf{p}_t, \mathbf{x}_t} \left\{ G_t(\mathbf{m}^n_t, \mathbf{p}_t, \mathbf{x}_t) + \overline{V}^{n-1}_t\left(\mathbf{m}^{a,n}_t\right) \right\} \tag{50}$$

$$\text{s.t. } (3), (5), (7), (10), (34)\text{–}(49).$$

Note that the concavity of the piecewise linear function is a favorable feature, since it allows the original one-stage bi-level model to be transformed into an equivalent single-level concave mixed-integer quadratic program (MIQP), which can be solved using the off-the-shelf MIQP solvers such as Gurobi or CPLEX.

After the one-stage subproblem (50) is solved, the VFA needs to be updated based on the marginal information of the current state $\mathbf{m}_t$, which can be referred to the benefit for having one more vehicle of a certain type. Here we can simply

use the solution to the dual variables associated with the resource capacity constraints, i.e., $\eta_{t,q}$, as the marginal value $\tilde{\mathbf{v}}_t^n$, and then update the VFA according to Eq. (A.1) in step 6 of Algorithm 1. Using dual values $\eta_{t,q}$ is also computationally favorable since they can be directly obtained by solving one-stage subproblem (50) in step 5 of Algorithm 1. Since only the VFA for a specific state is updated in each iteration, it is possible that the updated VFA may no longer preserve concavity. To maintain the concavity of piecewise linear function throughout the iterations, a so-called SPAR algorithm proposed by Powell et al. (2004) is applied to smoothen the updated VFA.

5. Numerical study

In this section, we evaluate the effectiveness of the proposed model and the ADP-based policy by running a series of experiments over both a small test example and a Chicago example. All numerical experiments are coded in Python and tested on a 2.2 GHz Intel i7 laptop with 16GB RAM. The transformed one-stage problem (50) is solved using Gurobi 7.5.1 with a solution time limit of 60 s.

The proposed dynamic pricing and vehicle dispatching policy is implemented via two steps: (i) training ADP-based policy using the approach in Section 4; and then (ii) decision making and performance evaluation based on the trained policy as well as real-time system states. In the training process, the vehicles and user ride requests are first simulated and then aggregated into vehicle and demand types at the beginning of each time period, so that VFA can be updated by solving the one-stage problem (50). This yields the prices for each candidate path, the vehicle dispatching decisions, and the vehicle-passenger matching decisions at the aggregated level. Then, the simulated individual ride requests are assigned to vehicles according to the aggregated plan until no available ride requests or vehicles exists. If a ride request can be matched to more than one vehicle, it would be assigned to its nearest designated vehicle based on the "first-come, first-serve" rule. Such a process is iterated until the terminal stage of the planning horizon. The performance of the ADP policy can be evaluated, using a process that is similar to the above training procedures except that the VFAs are no longer updated. Note that the procedures described above not only provide a better estimation of the system performance but also serves as a guideline of how to implement the proposed policy in the real world. For example, the training process can be conducted in an "off-line" sense, i.e., it can run for an arbitrary length of time over either a historical or simulated dataset, with the goal of obtaining a high-quality VFA. Meanwhile, to make real-time decisions, the most updated VFA can be implemented in an "online" sense by solving the one-stage problem (50) based on the current state of the system.

The numerical experiment settings are described as follows. We first partition the studied area into a set of small square zones with identical side length e. At each decision epoch, the company estimates the travel time for each path, which includes the in-vehicle travel time, the expected waiting time outside of the vehicle, and the expected detour time for picking up or dropping off other passengers. In fact, the travel time estimation itself is a separate research area (see Mori et al., 2015) beyond the primary focus of this study. To simplify the task, we make a few assumptions. The in-vehicle travel time is obtained by simply dividing the Manhattan distance between the centroids of origin and destination zones by the vehicle speed. The expected waiting time is estimated as the expected travel time from the centroid of the zone (where vehicles are expected to be) to a random passenger point in the same zone, i.e., $\frac{e}{2v}$. Estimating the expected detour time is rather complex since it depends on the balance between the supply and demand as well as the matching strategy. For simplicity, we assume the expected detour time at a certain zone z in time period t, denoted by $\tau_{t,z}$, is linearly proportional to the arrival rate of ride requests originating from zone z, i.e.,

$$\tau_{t,z} = \beta \sum_{\substack{r \in \mathcal{R}_t, \\ o_r = z}} \lambda_r, \ \forall z \in \mathcal{Z}, t \in \mathcal{T}, \tag{51}$$

where $\beta \geq 0$ is the associated coefficient. The rationale of this assumption is that the ridesharing is more likely to happen at the zones with a higher demand.

5.1. Hypothetical case

For insights, we first consider a hypothetical test case with 3×3 cells as shown in Fig. 4. The company operates 100 vehicles and attempts to optimize its pricing strategy in two 12-min time periods. Each vehicle is assumed to be able to carry at most two passengers and the vehicle speed is assumed to be 30 mph. The lower and upper bounds of the price are set to be 0 and 30, respectively. The monetary value of time is set to be $\alpha = 1$. The coefficient for detour time estimation in (51) is set to be $\beta = 1.0 \times 10^{-4}$. At the beginning of the time horizon, all of the 100 vehicles are idling at zone 7. For simplicity of illustration, we consider the deterministic demand for this hypothetical case. Specifically, in time period t, the ride requests from zone 7 to zone 9 and zone 7 to zone 1 have the maximum amounts of 33 and 28, respectively; in time period $t+1$, the ride requests from zone 8 to zone 9 has the maximum amount of 98. The price elasticity $B_r = 0.75$ for all types of demand. For comparison, we evaluate both the ADP and myopic policies for each test case under the same settings. The myopic policy is to solve a one-stage MIQP problem at each decision epoch without considering the VFA.

Table 1 presents the price, demand served and total revenue under the myopic and ADP policies, respectively. One can observe that, with myopic strategy, comparable prices are posted for path $7-8-9$ and path $7-4-1$ in the first time period so as to maximize the revenue in the current time period. However, when a large number of ride requests from zone 8 to zone 9 emerge in the second period, the myopic policy loses the opportunity of collecting more revenue from them

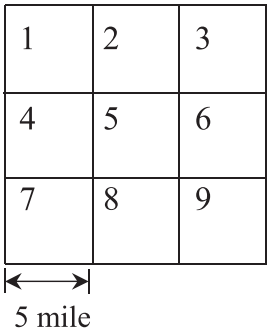

Fig. 4. Zone partition for the hypothetical example.

Table 1
Comparison results between ADP and myopic policy.

Time	Path	Price		Served demand		Revenue	
		Myopic	ADP	Myopic	ADP	Myopic	ADP
t	$7 \to 8 \to 9$	21.9	0.6	16	32	604	273
	$7 \to 4 \to 1$	18.1	18.1	14	14		
$t+1$	$8 \to 9$	30.0	30.0	16	32	480	960
Total	–	–	–	–	–	1084	1233

since most of the vehicles have already gone to zone 4 instead of zone 8 (due to the previous match of ride requests to path $7-4-1$ at a low price). In contrast, by applying the ADP policy, the company would post a relatively lower price for $7-8-9$ in the first period so as to encourage more travels through zone 7 to 9. This is reflected in the lower price and higher demand for path $7-8-9$ using ADP in time period t in Table 1. Then, in the second period, a higher portion of demand from zone 8 to zone 9 can share the vehicles with the riders that were originated in the first period while traveling from zone 7 to zone 9. In this way, the company is able to obtain a higher revenue in the second period by serving more ride requests. As shown in the last row of Table 1, the ADP policy can achieve 13.7% higher of total revenue compared to the myopic strategy. Therefore, by setting proper prices before the arrival of demand surges, the ADP policy significantly improves the system performance during the entire planning horizon. The main rationale behind this gain is that the ADP policy can take account the future information of the system into early decision-making processes by incorporating VFA, while the myopic pricing policy simply ignores such information, and therefore, the potential impacts of the current decision on the future states are not considered.

5.2. Chicago example

In this section, we further test the performance of the proposed modeling framework in a subarea of Chicago. As shown in Fig. 5, the test region is partitioned into 16 identical zones ($e = 2.5$ mile). We use the real data on Chicago taxi trips during 7:00 am–9:00 am on May 1, 2015 as the input.[6] The 2-h planning horizon is divided into eight periods (i.e., $\Delta =$ 15 min). To facilitate the demand generation process, we employ a concept of "zone-group", where a subset of nearby zones with similar land use patterns – e.g., central business districts (CBDs) or residential areas – share the same OD demand expectation. As in Fig. 5, the 16 zones are categorized into four zone-groups, including one CBD area and three residential areas (R1, R2, R3). Since the volume of taxi trips is relatively small in Chicago, we multiply the number of taxi trips with a coefficient $\kappa \geq 1$ for sensitivity analysis. Then, the simulated ride request data is generated through a Poisson process.

We generate 18 test instances by varying the total number of vehicles N, the price elasticities B_r and the demand scaling factor κ; i.e., $N \in \{320, 400, 480\}$, $B_r \in \{0.1, 0.5\}$ and $\kappa \in \{2, 3, 4\}$. At the beginning of the planning horizon, we assume empty vehicles are uniformly distributed in zones 1, 4, 5, 6, 7, 10, 14 and 15. The upper bound of prices is set to be \$25. The vehicle speed v is set to be 15 mph in this case. All other parameters are set to be the same as those in Section 5.1.

Convergence of the proposed algorithm is tested by evaluating the VFA during the ADP training process, using an identical set of sample paths across iterations. In so doing, simulations of demand are run for the current VFA after each training iteration, and then the sample average of the optimal total revenue throughout the entire planning horizon is computed across these simulations. The plot of this average vs. the iteration number for test case 5 ($N = 320, B_r = 0.5, \kappa = 3$) is shown in Fig. 6. We can observe that the proposed ADP-based algorithm seems to converge very fast, indicating that the VFA tends to stabilize only after a few iterations.

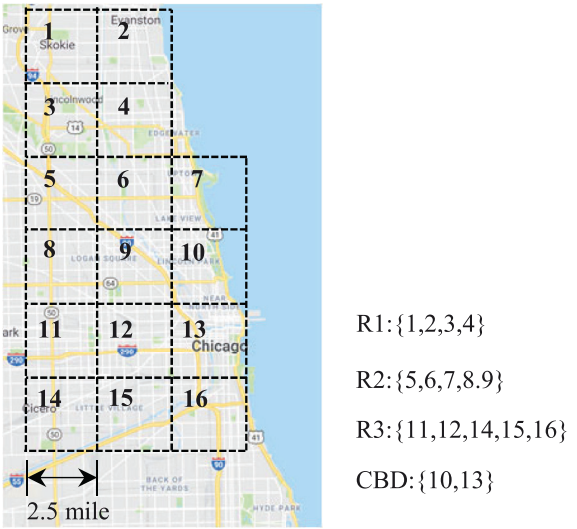

Fig. 5. Map of the Chicago example.

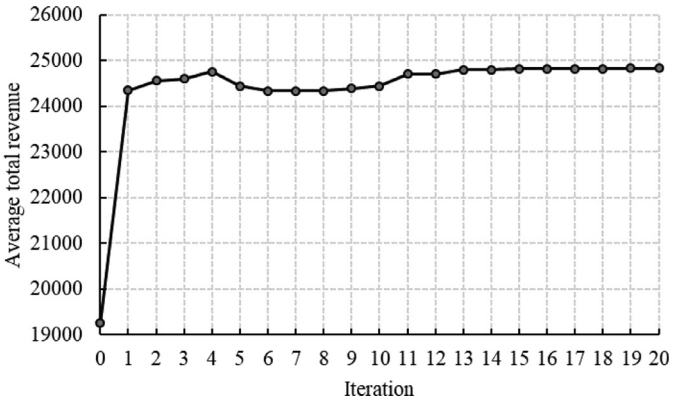

Fig. 6. Convergence pattern for the ADP algorithm ($N = 320, B_r = 0.5, \kappa = 3$).

Table 2
Comparison results for test cases of the Chicago example.

Case #	N	B_r	κ	Total revenue ($)			Improvement	
				ADP	Myopic	OD-based	VFA vs. Myopic	Path-based vs. OD-based
1	320	0.1	2	28,275	19,518	27,717	44.9%	2.0%
2	320	0.1	3	30,338	20,847	29,514	45.5%	2.8%
3	320	0.1	4	30,743	20,941	28,771	46.8%	6.9%
4	320	0.5	2	21,041	15,702	20,315	34.0%	3.6%
5	320	0.5	3	24,832	19,263	24,211	28.9%	2.6%
6	320	0.5	4	29,002	21,310	27,494	36.1%	5.5%
7	400	0.1	2	30,774	22,689	30,472	35.6%	1.0%
8	400	0.1	3	34,586	24,973	34,021	38.5%	1.7%
9	400	0.1	4	38,211	25,381	37,329	50.5%	2.4%
10	400	0.5	2	25,780	18,262	25,462	41.2%	1.2%
11	400	0.5	3	30,026	22,625	28,847	32.7%	4.1%
12	400	0.5	4	32,213	25,447	31,323	26.6%	2.8%
13	480	0.1	2	32,767	25,175	31,717	30.2%	3.3%
14	480	0.1	3	41,365	29,218	40,908	41.6%	1.1%
15	480	0.1	4	46,892	29,774	42,808	57.5%	9.5%
16	480	0.5	2	26,876	20,537	25,785	30.9%	4.2%
17	480	0.5	3	34,379	25,557	33,121	34.5%	3.8%
18	480	0.5	4	37,879	29,001	36,792	30.6%	3.0%

The results for all 18 test cases are shown in Table 2. For each case, we train the VFA for 20 iterations and then evaluate the performance of the trained policy by the average total revenue over another set of 20 random demand samples. We also apply our ADP model to an OD-based pricing scheme (in addition to myopic path-based pricing) to serve as another benchmark. The only difference between this OD-based and our path-based pricing strategies is that, for the OD-based one, we enforce identical prices for all the paths that share the same origin and destination zones at each decision epoch. Columns 5–7 of Table 2 present the sample-average total revenues under the path-based pricing strategy with VFA, the path-based myopic pricing strategy and the dynamic OD-based pricing strategy, respectively. The relative improvements achieved by applying the path-based pricing strategy with VFA are shown in the last two columns.

The results in Table 2 clearly show that the proposed ADP-based pricing policy (either path- or OD-based) outperforms the myopic counterpart in terms of maximizing the expected overall revenue for all the cases. In addition, it is easy to observe that when the demand level gets higher (with larger κ and smaller B_r) in dynamic settings, the merits of incorporating effective resource management strategies such as dynamic pricing and vehicle dispatching become more significant since the vehicles are likely to match and serve ridesharing passengers more effectively. Meanwhile, we can also observe that when the demand level is fixed, while the total expected revenue still increases with the vehicle number, the marginal benefit of increasing the fleet size actually diminishes. Taking test cases 4, 10, and 16 as an example, the total revenue increases by \$4739 when the fleet size goes from 320 to 400, while only by \$1096 when the number of vehicles goes from 400 to 480. A similar trend is also observed for all the other scenarios. As such, we can see that simply increasing the fleet size is not necessarily effective in resolving the spatiotemporal imbalance of ridesharing supply and demand. Moreover, we observe that the path-based dynamic pricing strategy holds the promise to generate better solutions than the dynamic OD-based counterpart. It should be noted that the shown benefits in our numerical cases are actually quite conservative since, the OD-based pricing policy tested here is not the current state of art – it still dynamically allows MSPs to manages resources across zones, which partially fulfilling the benefit from our path-based strategy.

6. Conclusion

This paper studies a dynamic pricing and vehicle dispatching problem to help ridesharing service providers address the imbalance between the vehicle resources and the spatiotemporally varying demand through optimal path-based pricing and vehicle dispatching decisions. The problem is considered as a dynamic Stackelberg leader-follower game and formulated as a multi-period MPEC model. A non-myopic ADP-based algorithm is developed with an embedded subroutine to transform the MPEC in each decision stage into a solvable MIQP. A series of numerical experiments are conducted to evaluate the effectiveness of the proposed model and to draw insights. It is shown that the ADP-based strategy is a promising way to improve the overall performance of ridesharing systems in stochastic and dynamic settings.

The work in this research can be extended in various directions. In the current study, we assume that once a route/price commitment is made to a passenger, it will be honored until the passenger arrives at his/her destination. However, if the traffic condition along the committed path changes significantly, the original commitment may no longer be suitable or realistic. Therefore, it would be interesting to investigate in the future how to design an even more “dynamic” pricing strategy to allow new options (as alternatives to the original commitment) to be proposed while the trip is already en-route. Moreover, we are also interested in looking into the interdependencies between roadway traffic congestion and the proposed path-based pricing strategy (when the ridesharing fleet is large enough to influence congestion), and trying to figure out how to make the optimal decisions if such endogenous interactions exist (similar efforts have been made in other contexts (e.g., Bai et al., 2014; Hajibabai et al., 2014; An et al., 2015; Hajibabai and Ouyang, 2016). Furthermore, in the proposed ADP algorithm, we use piece-wise linear functions to approximate the value function. It would be interesting to investigate whether the performance of the solution approach can be improved if other types of VFA, e.g., those based on neural networks, are used. Finally, this paper considers that the system consists of two stakeholders, MSP companies and riders, while some other players’ behaviors, such as the government and drivers, may also have impacts on the system performance. Thus, it would be an interesting topic to extend the current modeling framework to incorporate other stakeholders with different objectives and draw more managerial insights for ridesharing systems.

Acknowledgments

This research was supported in part by the U.S. National Science Foundation via Grants CMMI-1234085, CMMI-1662825, and a grant from the Zhejiang University - University of Illinois at Urbana-Champaign (UIUC) Institute Research Program. Very helpful comments from the three anonymous reviewers are also gratefully acknowledged.

[6] Source: https://data.cityofchicago.org/Transportation/Taxi-Trips/wrvz-psew.

Appendix A. Pseudocode for ADP

Algorithm 1 ADP algorithm.

Initialize $\overline{v}_t^0$ for all states $\mathbf{m_t}$ for $t \in T$
for $n = 1$ to N **do**
  Initialize the state of system m_0^n
  for $t = 0$ to $|\mathcal{T}|$ **do**
    Solve the one-stage subproblem with VFA.
    Obtain the marginal value information $\tilde{\mathbf{v}}_t^n$ and update the VFA based on (A.1):

$$\overline{v}_t^n(\mathbf{m}) = \begin{cases} \left(1-\theta^{n-1}\right)\overline{v}_t^{n-1}(\mathbf{m}) + \theta^{n-1}\tilde{\mathbf{v}}_t^n, & \text{for } \mathbf{m} = \mathbf{m}_t^n, \\ \overline{v}_t^{n-1}(\mathbf{m}), & \text{otherwise,} \end{cases} \tag{51}$$

    where $\overline{v}_t^n(\mathbf{m}_t)$ denotes the associated coefficients of $\overline{V}_t(\mathbf{m}_t)$, and $\theta^{n-1} \in [0,1]$ is the stepsize parameter.
    Update the state variable $\mathbf{m}_{t+1}^n$ according to Eq. (4). Update the stepsize θ^n by following a harmonic rule $\theta^n = \frac{1}{n+K}$, where training parameter K is an arbitrary positive integer.
  end for
end for

Appendix B. Reformulation of one-stage model

First, we present the reformulation of the bilinear term in (7) based on the derivations in Hobbs et al. (2000). By summing up (28) over $r \in \mathcal{R}_t, q \in \mathcal{Q}_{t,r}, k \in \mathcal{K}_{r,q}$, the bilinear term $\sum_{r\in\mathcal{R}_t}\sum_{q\in\mathcal{Q}_{t,r}}\sum_{k\in\mathcal{K}_{r,q}} p_{t,q,k}\cdot y_{r,q,k}$ can be written as follows:

$$\sum_{r\in\mathcal{R}_t}\sum_{q\in\mathcal{Q}_{t,r}}\sum_{k\in\mathcal{K}_{r,q}} p_{t,q,k}\cdot y_{r,q,k} = \sum_{r\in\mathcal{R}_t}\sum_{q\in\mathcal{Q}_{t,r}}\sum_{k\in\mathcal{K}_{r,q}} u_r\cdot y_{r,q,k} - \sum_{r\in\mathcal{R}_t}\sum_{q\in\mathcal{Q}_{t,r}}\sum_{k\in\mathcal{K}_{r,q}} \eta_{t,q}\cdot y_{r,q,k} - \sum_{r\in\mathcal{R}_t}\sum_{q\in\mathcal{Q}_{t,r}}\sum_{k\in\mathcal{K}_{r,q}} \alpha\cdot D_{r,q,k}\cdot y_{r,q,k}. \tag{B.1}$$

By summing up the market clearing constraints (10) and (29) over $r \in \mathcal{R}_t$, the first term on the right hand side can be reformulated as

$$\sum_{r\in\mathcal{R}_t}\sum_{q\in\mathcal{Q}_{t,r}}\sum_{k\in\mathcal{K}_{r,q}} u_r\cdot y_{r,q,k} = \sum_{r\in\mathcal{R}_t} H(u_r)\cdot u_r - \sum_{r\in\mathcal{R}_t}\Phi_{r,\zeta}\cdot y_{r,\zeta}. \tag{B.2}$$

The second term can be written equivalently written as

$$\sum_{q\in\mathcal{Q}_t}\sum_{r\in\mathcal{R}_{t,q}}\sum_{k\in\mathcal{K}_{r,q}} \eta_{t,q}\cdot y_{r,q,k} = \sum_{r\in\mathcal{R}_t}\sum_{q\in\mathcal{Q}_{t,r}}\sum_{k\in\mathcal{K}_{r,q}} \eta_{t,q}\cdot y_{r,q,k}, \tag{B.3}$$

where the right hand side of (B.3) can be reformulated into the following form by summing up (30) over $q \in \mathcal{Q}_t$:

$$\sum_{r\in\mathcal{R}_t}\sum_{q\in\mathcal{Q}_{t,r}}\sum_{k\in\mathcal{K}_{r,q}} \eta_{t,q}\cdot y_{r,q,k} = \sum_{q\in\mathcal{Q}_t} m_{t,q}\cdot\eta_{t,q}. \tag{B.4}$$

Given the assumption that $H(u)$ is a linear function of disutility u, we are able to reformulate the aforementioned bilinear term into a concave quadratic form by integrating (B.1)–(B.4), as presented in (35).

References

Agatz, N., Erera, A., Savelsbergh, M., Wang, X., 2012. Optimization for dynamic ride-sharing: a review. Eur. J. Oper. Res. 223 (2), 295–303.
Agatz, N.A.H., Erera, A.L., Savelsbergh, M.W.P., Wang, X., 2011. Dynamic ride-sharing: a simulation study in metro Atlanta. Transp. Res. Part B 45 (9), 1450–1464.
An, S., Cui, N., Bai, Y., Xie, W., Chen, M., Ouyang, Y., 2015. Reliable emergency service facility location under facility disruption, en-route congestion and in-facility queuing. Transp. Res. Part E 82, 199–216.
Bai, L., Mitchell, J.E., Pang, J.-S., 2012. On convex quadratic programs with linear complementarity constraints. Comput. Optim. Appl. 54 (3), 517–554.
Bai, Y., Kou, X., An, S., Ouyang, Y., Wang, J., Zhu, X., 2014. Integrated planning of tourism investment and transportation network design. Transp. Res. Rec. 2467 (1), 91–100.
Bai, Y., Ouyang, Y., Pang, J.-S., 2016. Enhanced models and improved solution for competitive biofuel supply chain design under land use constraints. Eur. J. Oper. Res. 249 (1), 281–297.
Banerjee, S., Riquelme, C., Johari, R., 2015. Pricing in Ride-Share Platforms: A Queueing-Theoretic Approach. Available at SSRN: https://ssrn.com/abstract=2568258
Bimpikis, K., Candogan, O., Saban, D., 2016. Spatial Pricing in Ride-Sharing Networks. Available at SSRN: https://ssrn.com/abstract=2868080
Cachon, G.P., Daniels, K.M., Lobel, R., 2017. The role of surge pricing on a service platform with self-scheduling capacity. Manuf. Serv. Oper. Manage. 19 (3), 368–384.
Campbell, P., Yang, Y., 2018. Didi Chuxing tests self-driving taxis on public roads https://www.ft.com/content/171e5d88-0f3c-11e8-8cb6-b9ccc4c4dbbb..
Caulfield, B., 2009. Estimating the environmental benefits of ride-sharing: a case study of Dublin. Transp. Res. Part D 14 (7), 527–531.
Chan, N.D., Shaheen, S.A., 2012. Ridesharing in North America: past, present, and future. Transp. Rev. 32 (1), 93–112.

Chen, M.K., Sheldon, M., 2015. Dynamic Pricing in a Labor Market: Surge Pricing and Flexible Work on the Uber Platform. Working Paper. University of California, Los Angeles.
Chen, X.M., Zahiri, M., Zhang, S., 2017. Understanding ridesplitting behavior of on-demand ride services: an ensemble learning approach. Transp. Res. Part C 76, 51–70.
Cortés, C.E., Matamala, M., Contardo, C., 2010. The pickup and delivery problem with transfers: formulation and a branch-and-cut solution method. Eur. J. Oper. Res. 200 (3), 711–724.
D'Acierno, L., Gallo, M., Montella, B., 2006. Optimisation models for the urban parking pricing problem. Transp. Policy 13 (1), 34–48.
Daganzo, C.F., 1994. The cell transmission model: a dynamic representation of highway traffic consistent with the hydrodynamic theory. Transp. Res. Part B 28 (4), 269–287.
Ell, K., 2018. Autonomous car ride-sharing service to launch in Texas https://www.cnbc.com/2018/05/07/autonomous-car-ride-sharing-service-to-launch-in-texas.html..
Fagnant, D.J., Kockelman, K.M., 2018. Dynamic ride-sharing and fleet sizing for a system of shared autonomous vehicles in Austin, Texas. Transportation 45 (1), 143–158.
Fellows, N.T., Pitfield, D.E., 2000. An economic and operational evaluation of urban car-sharing. Transp. Res. Part D 5 (1), 1–10.
Furuhata, M., Dessouky, M., Ordez, F., Brunet, M.-E., Wang, X., Koenig, S., 2013. Ridesharing: the state-of-the-art and future directions. Transp. Res. Part B 57, 28–46.
Gabriel, S.A., Leuthold, F.U., 2010. Solving discretely-constrained MPEC problems with applications in electric power markets. Energy Econ. 32 (1), 3–14.
Ghoseiri, K., 2012. Dynamic Rideshare Optimized Matching problem Ph.D. University of Maryland, College Park.
Hajibabai, L., Bai, Y., Ouyang, Y., 2014. Joint optimization of freight facility location and pavement infrastructure rehabilitation under network traffic equilibrium. Transp. Res. Part B 63, 38–52.
Hajibabai, L., Ouyang, Y., 2016. Planning of resource replenishment location for service trucks under network congestion and routing constraints. Transp. Res. Rec. 2567 (1), 10–17.
Hobbs, B., Metzler, C., Pang, J.-S., 2000. Strategic gaming analysis for electric power systems: an MPEC approach. IEEE Trans. Power Syst. 15 (2), 638–645.
Hosni, H., Naoum-Sawaya, J., Artail, H., 2014. The shared-taxi problem: formulation and solution methods. Transp. Res. Part B 70, 303–318.
Hu, J., Mitchell, J., Pang, J., Bennett, K., Kunapuli, G., 2008. On the global solution of linear programs with linear complementarity constraints. SIAM J. Optim. 19 (1), 445–471.
International Energy Agency, 2005. Saving Oil in a Hurry. OECD/IEA.
Jacobson, S.H., King, D.M., 2009. Fuel saving and ridesharing in the US: motivations, limitations, and opportunities. Transp. Res. Part D 14 (1), 14–21.
Korosec, K., 2017. Google's Waymo is launching a driverless ride-hailing service http://fortune.com/2017/11/07/google-waymo-phoenix-self-driving-car/..
Lee, A., Savelsbergh, M., 2015. Dynamic ridesharing: is there a role for dedicated drivers? Transp. Res. Part B 81, 483–497.
Lei, C., Ouyang, Y., 2017. Dynamic pricing and reservation for intelligent urban parking management. Transp. Res. Part C 77, 226–244.
Luo, Q., Saigal, R., 2017. Dynamic Pricing for On-Demand Ride-Sharing: A Continuous Approach. SSRN Scholarly Paper. Social Science Research Network, Rochester, NY.
Luo, Z.-Q., Pang, J.-S., Ralph, D., 1996. Mathematical Programs with Equilibrium Constraints. Cambridge University Press.
Mackowski, D., Bai, Y., Ouyang, Y., 2015. Parking space management via dynamic performance-based pricing. Transp. Res. Part C 59, 66–91.
Masoud, N., Jayakrishnan, R., 2017. A decomposition algorithm to solve the multi-hop Peer-to-Peer ride-matching problem. Transp. Res. Part B 99, 1–29.
Meyer, I., Kaniovski, S., Scheffran, J., 2012. Scenarios for regional passenger car fleets and their CO_2 emissions. Energy Policy 41, 66–74.
Mori, U., Mendiburu, A., Álvarez, M., Lozano, J.A., 2015. A review of travel time estimation and forecasting for advanced traveller information systems. Transportmetrica A 11 (2), 119–157.
Powell, W., Ruszczyński, A., Topaloglu, H., 2004. Learning algorithms for separable approximations of discrete stochastic optimization problems. Math. Oper. Res. 29 (4), 814–836.
Powell, W.B., 2011. Approximate Dynamic Programming: Solving the Curses of Dimensionality, 2nd ed. John Wiley & Sons, Hoboken, NJ.
Qiu, H., Li, R., Zhao, J., 2018. Dynamic pricing in shared mobility on demand service arXiv:1802.03559 [math]..
Santos, A., McGuckin, N., Nakamoto, H.Y., Gray, D., Liss, S., 2011. Summary of Travel Trends: 2009 National Household Travel Survey.
Sheffi, Y., 1985. Urban Transportation Networks: Equilibrium Analysis With Mathematical Programming Methods. Prentice Hall, Englewood Cliffs, N.J.
Shields, N., 2018. Lyft will start self-driving rides in Las Vegas this summer http://www.businessinsider.com/lyft-deploying-self-driving-bmws-in-las-vegas-2018-5..
Xie, W., Ouyang, Y., 2015. Optimal layout of transshipment facility locations on an infinite homogeneous plane. Transp. Res. Part B 75, 74–88.
Yang, H., Bell, M.G.H., 2001. Transport bilevel programming problems: recent methodological advances. Transp. Res. Part B 35 (1), 1–4.
Yu, B., Ma, Y., Xue, M., Tang, B., Wang, B., Yan, J., Wei, Y.-M., 2017. Environmental benefits from ridesharing: a case of Beijing. Appl. Energy 191, 141–152.
Zha, L., Yin, Y., Du, Y., 2017. Surge pricing and labor supply in the ride-sourcing market. Transp. Res. Procedia 23, 2–21.
Zha, L., Yin, Y., Xu, Z., 2018. Geometric matching and spatial pricing in ride-sourcing markets. Transp. Res. Part C 92, 58–75.